Metrol. Meas. Syst. Vol. XVI (2009), No. 1, pp. 117–127

PAN
POLSKA AKADEMIA NAUK

METROLOGY AND MEASUREMENT SYSTEMS
Index 330930, ISSN 0860-8229
www.metrology.pg.gda.pl

M&MS

A HELMHOLTZ COIL FOR HIGH FREQUENCY HIGH FIELD INTENSITY APPLICATIONS

Stefan Cirulo, Andrea Mariscotti, Angelo Vicava

University of Genoa, Elettrical Engineering Department, Via all'Opera Pia 11A, 16145 Genova, Italy (⊠ andrea.mariscotti@ unige.it, +39 01 035 32169, *stefano.cirulo@unige.it, angelo.vicava@unige.it)*

Abstract

In this work a general introduction to Helmholtz coil is presented and then attention is drawn to the implementation of a wideband (50 kHz) coil for applications requiring high magnetic flux density (up to a few mT) for sensor calibration, immunity tests and exposure of biological specimens. Experimental characterization confirms that field uniformity is quite good: dispersion is within 1.5% and 0.35% inside cubic volumes of 25% and 10% of the coil side respectively for the larger spacing; the measured impedance and the self resonance frequency are in accordance with the proposed simplified model; the magnetic field expanded uncertainty with k=2 is less than 0.5%.

Keywords: Helmholtz coils, magnetic measurements, calibration, uncertainty, stray capacitance.

1. Introduction

Generating fields of known and uniform strength is important in laboratory work. Such fields are necessary for accurate and repeatable immunity testing and also for equipment calibration.

Perhaps the simplest type of field generator seen is a planar coil. The magnetic field in the center of a circular coil is given by the formula $H = NI/2r$ where N is the number of turns, r the radius and I the current passed through the coil. The simple coil has its uses and its drawbacks. Simple coils are used in some EMC tests [1]-[3] to generate magnetic fields, either as small "field coils" placed next to the equipment under test (EUT), or in a larger "immersion" configuration. The benefits are simplicity of construction, small size and ease of installation; the drawback is non-uniformity of field: the field increases significantly at points near the wires and outside of the coil, the magnitude and direction of the field are sensitive to positioning and orientation.

There are several ways of producing a uniform magnetic field [4]: 1) a solenoid, 2) a toroid, 3) a spherical coil with variable winding, 4) a Helmholtz coil arrangement of stacked simple coils. The solenoid is a coil wound in a cylindrical fashion; for a

Article history: received on Jan. 31, 2009; accepted on Mar. 02, 2009; available on line on Mar. 18, 2009.

long and narrow solenoid the field in the center region is $H = NI/L$, where L is the length. A toroid is a solenoid wound around in a doughnut form so it closes on itself; the magnetic field is more uniform and it is still given by $H = NI/L$, where here L is the circumference of the toroid at the mean radius of the coil. There are two mechanical difficulties: size, because the toroid must be much larger than the equipment inserted into its interior, and accessibility, because the toroid is a closed surface that must be opened for insertion. The spherical coil is a sphere wound so that the sheet current density is proportional to the sine of the angle relative to the coil axis, a uniform field results throughout the entire volume of the sphere. A sinusoidally distributed sheet current can be approximated either by multiple windings driven through resistors of different values, or by varying the winding density over the surface of the sphere.

The standard geometry for a Helmholtz pair is two parallel coils spaced one radius apart and driven in phase [6]. Variation of the spacing over a fairly wide range has some effect on the field amplitude and uniformity; the Helmholtz coil can be constructed with either circular or square coils and this choice has a slight influence on field uniformity as well. The field it generates is the sum of the fields generated by the two spaced coils; the surprisingly large volume of field uniformity results because there is a good deal of cancellation for the off -axis field components generated by the coil.

The advantage of Helmholtz coils is that they have a simple geometry (with respect to configuration 3) and they allow large equipment to be fit within the two coils, that is impossible for all other solutions.

The rectangular geometry is convenient, especially for construction and installation. Single square coils have been used for calibration of extremely low frequency magnetic field meters for applications that require uncertainties of a few percent [5][11]. Multiple rectangular loops with a common axis have found applications in a number of fields, including biological exposure systems for in vivo and in vitro studies [4][5]. It is also noteworthy that a square Helmholtz coil produces a greater volume of nearly uniform magnetic field than a circular Helmholtz coil of comparable dimensions.

Finally, it is to be underlined that immunity standards [2][3] require single (or few) turn coils not only for high frequency but also for supply frequency testing. If this requirement is very important to the limit stray capacitance and resonance effects at high frequency, it really asks for a high current capability amplifier or generator at low frequency. The presented design and implementation is a viable solution to keep the required current amplitude low, while ensuring a large bandwidth (above 50 kHz). The proposed Helmholtz coils have been used to perform magnetic field immunity tests on Intelligent Positioners, industrial equipment of not negligible size for the control of valve actuators [7].

The optimization and use of a Helmholtz coils pair over an extended frequency range were also considered in [8] as an efficient alternative method with respect to that described in[9].

It must be reminded that there are secondary effects that limit the high frequency performance of Helmholtz coils [6][8]: a) fall-off of the input current vs. frequency if the coil is supplied by a voltage source; b) parallel resonance of coil inductance and stray capacitance, that increases input impedance and makes the coil difficult to drive; c) for higher frequency values the distributed nature of the coil comes into play and reactive modes appear along coil circumference up to the limiting frequency at about one tenth of the total wire length.

Series connection of the Helmholtz coils ensures the same current in the two coils and the need for only one driving source; for this configuration the self resonance frequency may be estimated as

$$f_r = \frac{1}{2\pi\sqrt{(L+M)(C+C_g)}}, \tag{1}$$

L and M are the self and mutual inductance of the coils, C is the stray inter-turn and inter-winding capacitance and C_g is the stray capacitance to ground (made negligible by keeping the lower side of the coils 1 m above the floor on a wood table). This relationship will be used to verify the experimentally measured resonance frequency.

2. Field equations and theoretical characterization

Only some expressions are reported to ease the analysis of the Helmholtz coil and the optimization of geometric parameters, while keeping the size of the theoretical framework as small as possible. A very accurate and complete treatment may be found – among others – in a report written by K. Kuns [10]. A pioneering work is that of Lin and Kaufmann [11], who report also an expression that account for the self heating effect on the uniformity of current density along the coil.

More simply, for a single square coil of side $2a$ and $2b$, N turns and input current I, one can obtain the field B_z on coils axis by application of the Biot-Savart law and integration [13]

$$\begin{aligned} B_z &= NI\frac{\mu_0}{4\pi}\sum_{n=1}^{4}\frac{(-1)^n D_n}{r_n[r_n+(-1)^{n+1}C_n]} - \frac{C_n}{r_n(r_n+D_n)} \\ \text{where } & C_1 = -C_4 = a+x \quad C_2 = -C_3 = a-x \\ & D_1 = D_2 = b+y \quad D_3 = D_4 = -b+y \\ & r_1 = \sqrt{(a+x)^2+(b+y)^2+z^2} \quad r_2 = \sqrt{(a-x)^2+(b+y)^2+z^2} \\ & r_3 = \sqrt{(a-x)^2+(b-y)^2+z^2} \quad r_4 = \sqrt{(a+x)^2+(b-y)^2+z^2} \end{aligned} \tag{2}$$

With attention to the coordinate system with its origin in the center of the first coil and orientation of z along coil axis (see Fig. 1 below), one can add the second coil with the coordinated translation by d (coil spacing) and bring the second derivative to x of the total field (with $a = b$ in our case) to zero, to obtain the solution for maximum flatness $d \cong 1.07a$, in accordance with the value of 1.057 reported in [11]. It is observed that most often when an optimal separation is calculated for field uniformity, the calculation is done with respect to the central field value; if the average and the sum of squares of difference of field values in a given region of space are considered, without taking the central value as the reference value, the solution may be slightly different. Numerical simulations for larger separation indicate that a similar uniformity may be obtained as well, but only on reduced volumes (see at the end of Section IV).

Bronaugh [6] reports a useful formula (for circular coils) to locate the major sources of field error.

$$\frac{\delta B}{B} = -0.2\,(\delta r_1/r_1 + \delta r_2/r_2) - 0.6\delta d/d + \delta I/I + \delta N/N. \tag{3}$$

The most important terms are $\delta I/I$ and $\delta N/N$, that are the relative errors on the input current and number of turns: the first may be made very small in the order of the accuracy of the shunt used for the measurement (about ±0.1% over the entire frequency range, since stray capacitance and inductance terms are not relevant for a resistance value in the order of a fraction of Ω) and of the measuring instrument connected to the shunt (from about 0.3% for an 8 bit oscilloscope down to much less than ±0.1% for sampling voltmeters and high resolution digital acquisition boards). The second term may be excluded since the number of turns is exact (128 in our application). The coil frame is made of plywood with reinforcement wood patches and bars; the machining tolerance is below 1 mm for edges, profiles and holes and we may estimate an equivalent size relative error of ±0.5 mm / 520 mm (half the average side length of each coil, that gives a ±0.2% error uniformly distributed). Spacing is controlled twice before each test on all sides of the parallelepiped and in this case the error is related to the reading error on a mm scale, roughly about ±0.5 mm over 500-800 mm (relative error of approx. ±0.16% uniformly distributed). The calculated maximum expanded ($k = 2$) uncertainty is approx. 0.47%, or 0.32% without the influence of the voltage measurement.

3. Coil design

Helmholtz coils are square with 1 m nominal side length. To account for the effective winding thickness, made of eight layers of 3 mm thickness each, the internal side length was set to 0.98 m, so that the average side length is approximately 1 m. Each coil is composed of $N_t = 16$ turns and $N_l = 8$ layers.

Winding geometry was designed to minimize stray capacitance. The analysis of inter-turn stray capacitance C_t and inter-layer stray capacitance C_l terms suggest that the most important term of the total coil capacitance C_c is C_l: because of the Miller effect C_l for each turn pair is increased approximately by the ratio of the effective voltage difference between two turns on adjacent layers V_{ll} and the voltage difference between two adjacent turns in the same layer V_t.

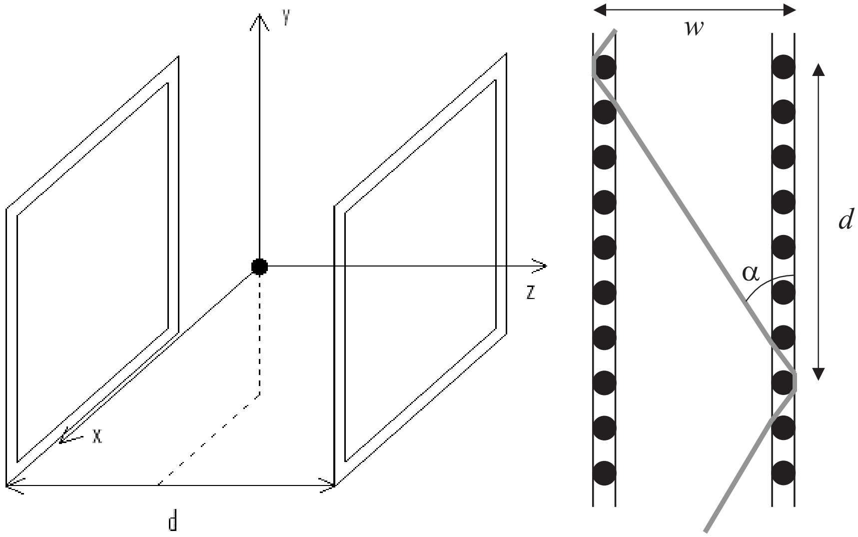

Fig. 1. Helmholtz coil geometry with coordinate system and pattern of the single layer.

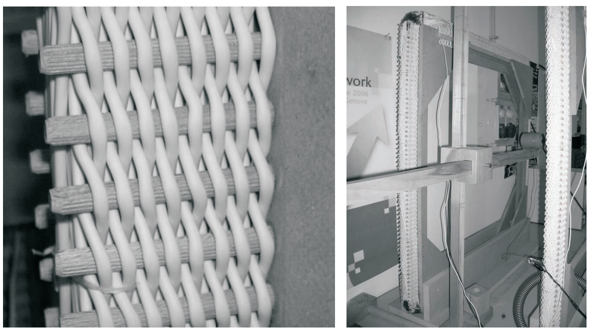

Fig. 2. Construction of the Zig zag winding and final implementation with the positioning system.

The winding structure is as shown in Fig. 1 and 2: the turn is wound with a zig-zag path; the skew angle α can be computed from the pitch d and the winding width w. The total turn length L_t is $d/\cos\alpha$, and for usual values of α (about 20-25°) this represents an increase with respect to the straight length d of the frame of about 6-10%. In our case 128 turns with an average perimeter of 4.16 m took about 585 m of wire for each coil. The turn resistance R_t (and so the total coil resistance R_c) is a linear function of turn length and cross section ratio; it was found for both coils $R_c = 8.30 \pm 0.11\Omega$, in accordance with the 1.25 mm^2 cross section of the used wire.

Coil inductance and capacitance measured at input terminals are $L_1 = 43.8 \pm 0.8$ mH and $L_2 = 43.3 \pm 0.8$ mH, $C_1 = 170 \pm 10$ pF and $C_2 = 176 \pm 10$ pF respectively for the two coils. The stray capacitance was determined based on the measurement of the single coil self-resonance, found at 61.8±0.1 kHz for both coils. The mutual inductance M between coils depends on coils separation between coils; if the expression reported in [8] (valid only for one unstated distance and for circular coils) is considered, the calculated resonance frequency of the pair is 55.1 kHz, that is quite close to the measured one (see next Section).

Coil inductance is not an issue for large field tests at a single frequency at each time, since inductive reactance can be almost canceled out by the series capacitive reactance of the tuning capacitor bank, reaching magnetic field levels well above 1 mT at audiofrequency. Transient field tests or fast sweeping field tests may be accomplished by means of a current source amplifier or a high voltage source followed by a large series resistor (much larger than the coils inductive reactance), because of field uniformity with respect to frequency (see next Section). With these feeding techniques it is possible to observe that any change of winding resistance is of no effect; however, it is easy to see that with a wire radius of 0.6 mm (corresponding to the above – stated cross section), there is no appreciable skin effect up to 10 kHz and skin depth at 50 kHz is only 50% of the radius itself.

4. Experimental characterization

In addition to the determination of the basic electrical parameters of the two coils, series of measurements have been done in order to: first, define the coil input impedance Z_c; second, check the uniformity of bulk current I_b (the sum of the currents in the individual wires, as defined in [14]) with respect to the input current I_i; third, evaluate magnetic field level and uniformity, with the definition of regions of space of given field uniformity, where experimental values are compared with those derived from magnetic field equations (referred to as "theoretical values").

The coil impedance Z_c has been measured with a voltamperometric method: the results have been partially reported at the end of Section III to illustrate coil design; the input current for constant applied voltage, inversely proportional to Z_c, is shown in Fig. 3.

Uniformity of the bulk current was qualitatively checked by moving a Rogowski coil along the coil perimeter and no appreciable difference was detected (within approximately 1%, so within the sensitivity of Rogowski to displacement of the central current carrying conductor). A Rogowski coil with improved common - mode and external electric field rejection [15] has been used too and it confirmed the first measurement results up to the resonance frequency. It is possible to show that the usability of the Helmholtz pair as a magnetic field source is up to and above the main input resonance, since the bulk current exhibits a much larger uniformity than the input current at these frequencies [14].

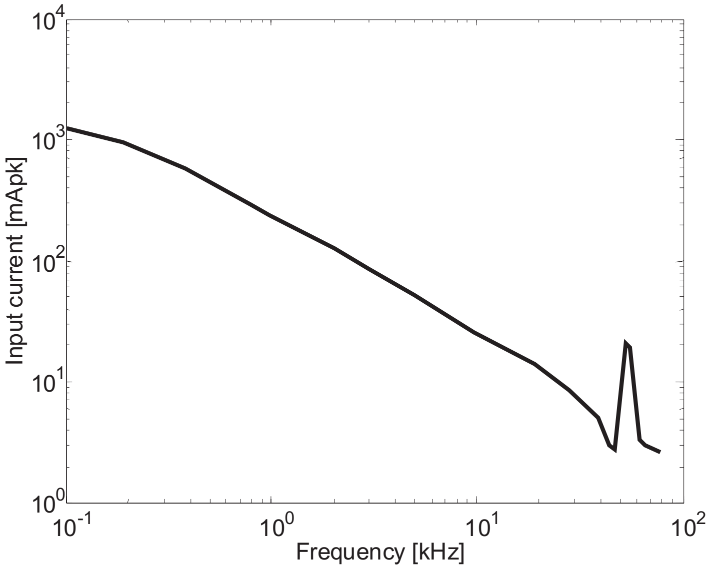

Fig. 3. Coil input current vs. frequency (measured).

Magnetic field uniformity was tested for different coil separations *d*, operating frequencies (attention is focused on 55 kHz, a very high value close to coil resonance, and a smaller value, 10 kHz, representing low frequency behavior) and positions with respect to the coil center.

Other tests at lower frequency values have shown that, excluding the small uncertainty related to the search of the resonance frequency for each capacitor bank configuration, the flatness of the frequency response is within about 0.3%.

Some sample test results are shown in Fig.4 to illustrate the activity. Two coil spacing values (found in the literature as suggested optimal values) have been investigated: 80 cm (indicated by the CENELEC standards [2][3]) and 60 cm (found as indicated in Section II); the field values are normalized per 1 A of bulk current. The magnetic field B is measured with a small search coil with 8 spaced turns, eccentricity <1.5%

and calibrated by construction; yet, the positioning system is contributing the largest uncertainty to the measured values.

For d=80 cm spacing (Fig. 4a) it can be observed that in the central portion of space the B field is very uniform and attention is concentrated on a cubic space of 11 cm side (5.5 cm in the half plane plots), where any magnetic field sensor may be placed for calibration. The average field B_{av}=1.0942 μ T/A and the dispersion is 2%. If the considered portion of space is now a sphere (that fits much better the shape of the majority of magnetic field sensors [16][17]) with a diameter of 11 cm, the average field increase slightly to 1.1032 μ T/A, but the dispersion reduces to 0.5%.

Field uniformity is even better for d=60 cm (Fig. 4b) over the considered cubic space (11 cm side): B_{av}=1.4178 μ T/A and the dispersion is 0.35%; for the sphere with diameter of 11 cm, B_{av}=1.4162 μ T/A and the dispersion is still 0.35%. This clearly ensures a better uniformity with respect to larger spacing, and a 35% higher field (if the average field values are considered). It is worth to underline that the maximum spread of values,*i.e.* $B_{max} - B_{min}$ vs. the average field is only 2.33% for 60 cm.

If the coil set is to be used for immunity tests, then the requirements on field uniformity are much less stringent, since 1 to 3 dB are usually required, thus between approximately 10% and 30%; a much larger space may be used then and the coil separation may also be increased to accommodate for very large objects, close to the coil separation itself. For these applications it was found in [7] that 50 Hz field uniformity in terms of maximum spread was better than 25%.

The Type B uncertainty can be calculated from (3), from the declared uncertainties of used measuring equipment and from the assumed errors in positioning and geometry of the search coil: the $k = 2$ expanded uncertainty is around 1.16% for the 8 bit acquisition system. The direct evaluation of Type A uncertainty with $k = 2$ from repeated measurements (9 for each point in space) excludes the errors in the positioning of the search coil, but includes the contribution of the channel of the acquisition system connected to the search coil; it is <0.5% for all points and, if depurated of this additional uncertainty term, it is very close to the one computed at the end of Section II.

A significant series of independent tests is not available at the moment to estimate the reproducibility, taking into account different environmental conditions (especially temperature and humidity, taking into account that the coil supports and the positioning system is made of wood). However this is out of the scope of the presented system, since the replacement of wood with a suitable plastic material (such as polyvinyl chloride or nylon) would reduce the most significant term of the uncertainty budget: geometry tolerances and positioning errors.

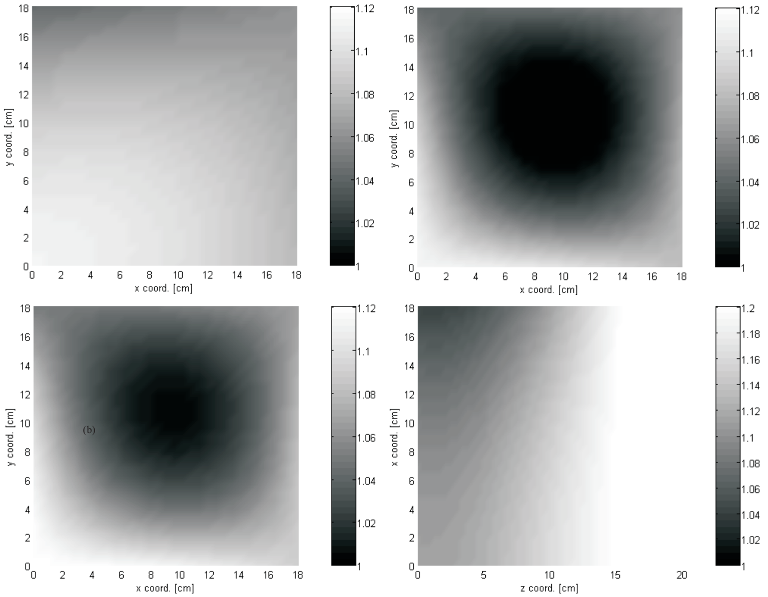

(a)

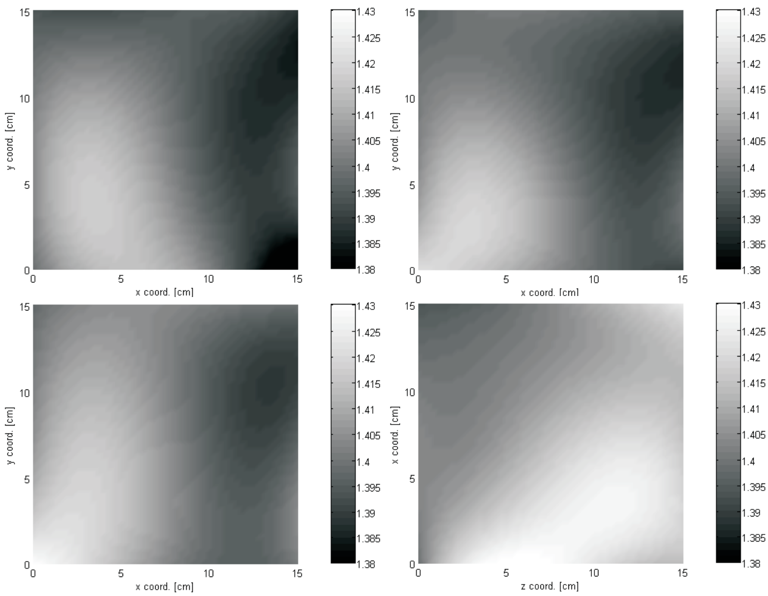

(b)

Fig. 4. Measured values of B_z [μT] / I_b [A] for coil spacing of (a) <u>80 cm</u>, (b) <u>60 cm</u>: z=0 cm (upper left), z=2 cm (upper right), z=4 cm (lower left) and y=0 cm (lower right).

5. Conclusions

The main elements for the construction of a wideband Helmholtz coil pair and related test results have been presented and discussed. The target applications are: magnetic field immunity testing of equipment of considerable size, the application of fairly constant and uniform magnetic field to laboratory specimen (such as during biological experiments) and finally the calibration of magnetic field sensors with a satisfactory field uniformity and repeatability within a fraction of % for a wide range of sensor size. The Helmholtz coil is attractive with respect to solenoids and similar architectures because it is an open architecture that does not impose constraints on the geometry of the device under test, so that one equipment fits several applications with a very satisfactory accuracy.

References

[1] MIL STD 461E, *Requirements for the control of Electromagnetic Interference Characteristics of Subsystems and Equipment*, 1999–08.

[2] EN 61000-4-8, *Electromagnetic compatibility (EMC) – Part 4: Testing and measurement techniques. Section 8: Power frequency magnetic field immunity test – Basic EMC publication*, 1993–09.

[3] EN 61000-4-9, *Electromagnetic compatibility (EMC) – Part 4: Testing and measurement techniques. Section 9: Pulse magnetic field immunity test – Basic EMC publication*, 1993-09.

[4] I. Straus: *Magnetic field calibration: unwinding the Helmholtz coil. Conformity*, May 2002, pp. 40–44 *www.confirmity.com*.

[5] M. Misakian: "Equations for the Magnetic Field Produced by One or More Rectangular Loops of Wire in the Same Plane". *Journal Research NIST*, vol. 105 no. 4, July/Aug. 2000, pp. 557–564.

[6] E.L. Bronaugh: "Helmholtz coils for calibration of probes and sensors: limits of magnetic field accuracy and uniformity". *IEEE Intern. Symp. on Electromagnetic Compatibility*, 1995, pp. 72–76.

[7] M. Caserza Magro, A. Mariscotti, P. Pinceti: "EMC testing of Fieldbus interconnected Intelligent Positioners". *Instrumentation and Measurement Technology Conf. IMTC 2006*, Sorrento, Italy, April 20–23, 2006.

[8] E.R. Javor, T. Anderson: "Design of a Helmholtz coil for low frequency magnetic field susceptibility testing". *IEEE Intern. Symp. on Electromagnetic Compatibility*, 1998, pp. 912–917.

[9] MIL STD 461E, *Requirements for the control of Electromagnetic Interference Characteristics of Subsystems and Equipment*, 1999–08.

[10] K. Kuns: "Calculation of Magnetic Field Inside Plasma Chamber", *UCLA report*, Aug. 14, 2007. Online *http://plasmalab.pbwiki.com/f/bfield.pdf* .

[11] S.T. Lin, A.R. Kaufmann: Helmholtz Coils for Production of Powerful and Uniform Fields and Gradients, *Review of Modern Physics*, vol. 25 no. 1, Jan. 1953, pp. 182–190.

[12] IEEE Std. 291, *IEEE standard methods for measuring electromagnetic field strength of sinusoidal continuous waves, 30 Hz to 30 GHz*, 1991.

[13] IEEE Std. 644, *IEEE standard procedures for measurement of power frequency electric and magnetic fields from AC power lines*, 1994.

[14] C. Carobbi, S. Lazzerini, L. Millanta: "High frequency operation of the coils for standard magnetic field generation using the bulk-current technique". *IEEE Transactions on Instrumentation and Measurements*, vol. 54 no. 4, Aug. 2005, pp. 1427–1432.

[15] A. Mariscotti: "A Rogowski coil for high voltage applications", *International Instrumentation and Measurement Technology Conf.* I^2*MTC*, Victoria, Vancouver Island, Canada 12–15 May 2008.

[16] IEEE Std. 1140, *IEEE Standard Procedures for the Measurement of Electric and Magnetic Fields from Video Display Terminals (VDTs) from 5 Hz to 400 kHz*, 1994.

[17] A. Mariscotti: "A Large Bandwidth and Dynamic Range Magnetic Field Probe", *Instrumentation and Measurement Technology Conf. IMTC 2007*, Warsaw, Poland, May 2–4, 2007.